F-AM-H1 MECHANISM OF POSTREPLICATION REPAIR IN HAEMOPHILUS INFLUENZAE. Gary D. Small* (Intro. by F. W. Studier), Biology Department, Brookhaven National Laboratory, Upton, New York 11973.

DNA pulse labeled following ultraviolet irradiation of excision defective mutants of H. influenzae is of lower single strand molecular weight than that of unirradiated cells but approaches the size of DNA from unirradiated cells upon further incubation in growth medium. This gap-filling process is controlled by the recl gene. Gap-filling occurred normally in a temperature-sensitive DNA synthesis mutant at the restrictive temperature showing that normal semiconservative DNA synthesis is not necessary for gap filling. To test for recombinational events following irradiation, the DNA synthesized after irradiation was pulse labeled in medium containing 5-bromodeoxyuridine (BrdUrd) followed by incubation for various times in nonradioactive, BrdUrd-containing medium. The DNA was denatured and analyzed isopycnically. The labeled DNA was initially "heavy", but later shifted toward ligher densities. This shift occurred in the temperature-sensitive DNA synthesis mutant at the restrictive temperature but was not seen in the recl mutant. The density shift can be interpreted as evidence that rather extensive exchanges occurred between parental DNA and the DNA made after irradiation. These results suggest that such exchanges are important for gap filling in H. influenzae. Research carried out at Brookhaven National Laboratory under the auspices of the U. S. Atomic Energy Commission.

F-AM-H2 THE EFFICIENCY OF EXCISION REPAIR AND CELL SURVIVAL IN YEAST. R.H. Haynes, Department of Biology, York University, Toronto, Ontario, R. Wheatcroft* and B.S. Cox*, Botany School, University of Oxford, England.

It can be shown theoretically that an initial shoulder should exist on radiation survival curves for cells in which the efficiency of repair of potentially lethal lesions declines with increasing dose. Wild-type strains of the yeast Saccharomyces cerevisiae are capable of excising UV-induced pyrimedine dimers from their DNA. In addition, at least two other pathways for DNA repair exist in this organism. Measurements of the ratio of dimers excised to dimers induced over the dose range 2000-12,000 ergs/mm^2 show that the efficiency of this mode of repair does indeed decline with increasing UV dose to the cells. Furthermore, a reasonable extrapolation of the efficiency data into the 'low dose' survival range indicates that the biochemical and survival measurements are quantitatively coherent within the context of theory mentioned above. That is, the wild-type survival curve can be predicted with reasonable accuracy on the basis of data on excision efficiency and the UV sensitivity of excision deficient mutants. (Work supported by grants from the National Research Council of Canada and the Science Research Council of the United Kingdom).

F-AM-H3 The Characterization of an Exonuclease Purified from Human Placenta Capable of Pyrimidine Dimer Excision.
J. Doniger* and L. Grossman, Graduate Department of Biochemistry, Brandeis University, Waltham, Massachusetts 02154.

An exonuclease has been purified from human placenta which is active on single-stranded DNA, but not on native DNA. Since single-stranded circular ϕX174 DNA is not hydrolyzed, the enzyme is characterized as an exonuclease. The enzyme is able to act on duplex DNA which has extending single-stranded termini. It hydrolyzes at both 3' and 5' termini with equal facility, releasing oligonucleotides with 5'-phosphorylated termini. Oligonucleotides predominantly 4-7 residues in length are produced, irrespective of the terminus from which hydrolysis is initiated. The exonuclease specifically excises pyrimidine dimers from ultraviolet irradiated DNA incised by a UV-specific endonuclease isolated from Micrococcus luteus. This suggests that this enzyme has the potential for involvement in DNA repair in human tissues.

F-AM-H4 POST-REPLICATION REPAIR IN UV-IRRADIATED *tsl-1* DERIVATIVES OF *lexA3* MUTANTS OF *ESCHERICHIA COLI K-12*.
Ann K. Ganesan, David W. Mount* and Patricia C. Seawell*. Department of Biological Sciences, Stanford University, Stanford, California 94305; and Department of Microbiology, College of Medicine, University of Arizona, Tucson, Arizona 85724.

The *lexA* mutations of *E. coli K-12* are dominant mutations which decrease cell survival after UV irradiation, but do not diminish genetic recombination in otherwise wild-type cells. The *tsl-1* mutation, originally isolated as a suppressor of the *lexA3* mutation, restores cell survival after UV irradiation to wild-type levels. We have compared post-replication repair in *lex*$^+$, *lexA3* and *tsl-1* cells. For these experiments thymine-requiring cultures were grown with ^{3}H-thymidine for 10 minutes after a dose of 4 J/m^2 nm. Samples were taken from the cultures either immediately following removal of the ^{3}H-thymidine or after 20 minutes growth in non-radioactive medium. The cells were lysed and the DNA was analysed on alkaline sucrose gradients. In all cases the labeled DNA from irradiated cells sampled immediately after removal of the ^{3}H-thymidine sedimented more slowly than DNA from unirradiated controls. After 20 minutes growth in non-radioactive medium, labeled DNA from irradiated *lex*$^+$ and *tsl-1* cells sedimented as rapidly as the DNA from unirradiated controls. However, the labeled DNA from *lexA3* cells still sedimented more slowly than control DNA. From these results we concluded that *lexA* mutations interfere with post-replication repair in UV-irradiated cells, inhibiting the conversion of low molecular weight DNA to high molecular weight, while the *tsl-1* mutation reverses this inhibition.

This work was supported by grant GM 19010 from NIH, contract AT(04-3)326-7 from AEC, and grant GB 27910 from NSF.

F-AM-H5 PARTIAL PURIFICATION FROM HUMAN LYMPHOBLASTS OF ENDONUCLEASES FOR DAMAGED DNA. Thomas P. Brent, St. Jude Children's Research Hospital, Memphis, Tennessee 38101.

Crude extracts of cultured human lymphoblasts (CCRF-CEM cells) contain endonuclease activity that cleaves UV-irradiated DNA in preference to untreated DNA. Attempts to purify this activity utilized UV-irradiated PM2 phage DNA (5000 ergs/mm^2) as substrate in the enzyme assay. Since endonuclease specific for depurinated and depyrimidinated DNA might account for the apparent UV-DNA specific activity, fractions derived during the purification were also assayed with PM2 DNA partially depurinated by heating to 70°C at pH 5 for 8 min. Elution of a 45-60% ammonium sulphate fraction from G-100 Sephadex yielded a peak of activity for UV-DNA equivalent to about 35,000 daltons. This peak was highly active with depurinated DNA. Further purification on a DEAE-cellulose column resolved two major peaks of activity. Peak 1, detected by assay with depurinated DNA, showed only traces of activity for UV- or untreated DNA, and was strongly stimulated by Mg^{++}. Peak 2, detected by assay against UV-DNA, was equally active with untreated DNA and was inhibited 2-fold by Mg^{++}. The low level of activity for UV-DNA in Peak 1 suggests that this endonuclease is not responsible for the preferential activity for UV-DNA seen in crude extracts. Additional studies indicate the presence of a third activity which is specific for UV-DNA but is extremely labile during purification. This might be the UV-specific endonuclease activity detected in crude extracts.

Supported by DRG-1223 from Damon Runyon Memorial Fund for Cancer Research, CA-14799 from National Cancer Institute and by ALSAC.

F-AM-H6 PARTIAL PURIFICATION FROM YEAST OF AN ACTIVATOR AND AN INHIBITOR OF DNA PHOTOLYASE. J.J. Madden* and H. Werbin* (Intr. by John Jagger), Institute for Molecular Biology, The University of Texas at Dallas, P.O. Box 688, Richardson, Texas 75080.

Minato and Werbin (Physiol. Chem. & Physics 4, 467 (1972)) extracted from yeast a crude fraction which enhanced the photoreactivation ability of highly purified DNA photolyase, and suggested that this extract a co-factor which acted as the chromophore for the enzyme. We have further purified this material by ion-exchange chromatography and gel-filtration and have isolated from it two components, which affect the enzyme's activity, one an inhibitor and the other an activator. The inhibitor, which was homogeneous in two thin-layer chromatography systems, has fluorescent excitation maxima at 295 nm and 375 nm, and emission maxima at 350 nm and 480 nm. The inhibitor can completely abolish enzyme activity at low inhibitor-enzyme ratios, suggesting a high degree of specificity of the inhibition. The activator appears to be a small polypeptide of slightly higher molecular weight than the inhibitor (approximately 1000 daltons vs. 600 daltons respectively, determined by gel filtration). This work was supported by A.E.C. Contract #AT-(40-1)-3630 and by Robert A Welch Foundation Grant #AT-480.

F-AM-H7 DETECTION OF POLY A, POLY U AND POLY C HYDROLYSIS BY LIGHT SCATTERING.

John W. Preiss and Martin F. Brady*, Department of Physics, The University of Delaware, Newark, Delaware 19711.

In weakly acidic solutions, pancreatic ribonuclease catalyzes a very slow hydrodysis of poly A. During this process enormous loosely-bound poly A-ribonuclease clusters form, grow in size and eventually collapse. These are very easily studied by light scattering techniques. This phenomenon is not observed with poly U or poly C because the hydrolysis is too rapid. One can get around this by mixing either of these homopolymers with poly A before adding the ribonuclease. This slows the rate at which poly A is hydrolyzed because the poly U and poly C become entangled in the clusters. One can detect as little as 3 μg/mℓ of poly U in the presence of 15 μg/mℓ of ribonuclease, if the reaction is carried out at temperatures below 18°C. The behaviour with poly U is different from that with poly C because of base pairing with poly A.

F-AM-H8 DEGRADATION OF MS II (pppGpp) IN E. COLI

Kreurvul Sophasan* and R.C. Bockrath, Dept. of Microbiology, Indiana University School of Medicine, Indianapolis, Indiana 46202.

Several slow-growing mutant strains of Escherichia coli were assayed for steady-state levels of 3'-diphosphate, 5'-diphosphate guanosine (MS I or ppGpp) and 3'-triphosphate, 5'-diphosphate guanosine (MS II or pppGpp). Mutant strain W-61 contained an unusually high level of MS II. Sucrose-washed ribosomes from this strain, and from the parent strain WWU, were compared in vitro. Using ATP and GTP as substrates, both preparations mediated the synthesis of ppGpp and pppGpp, but the time course kinetics were clearly different. With ribosomes from the parent strain the apparent equilibrium level for ppGpp was considerably greater than that for pppGpp (analogous to in vivo results for WWU). With ribosomes from the mutant strain the levels of ppGpp and pppGpp were nearly identical (analogous to in vivo results for W-61). Using ppGpp and pppGpp as substrates, both preparations of ribosomes mediated degradation of pppGpp but ribosomes from the parent strain indicated a greater specific activity. There was no degradation of ppGpp. Further, ribosomes from mutant W-61 supplemented with the high salt wash of ribosomes from WWU caused rapid degradation of pppGpp, whereas the same ribosomes supplemented with salt-washed ribosomes from WWU produced slow degradation of pppGpp. When labelled pppGpp was prepared from α-^{32}P-GTP, degradation of pppGpp was accompanied by an increase in labelled GDP. These results suggest a ribosome associated degradation mechanism for MS II in E. coli which may be defective in a mutant such as W-61.

This work was initiated by R.C.B. during a visit with Prof. N.O. Kjeldgaard, Institute for Molecular Biology, Aarhus, Denmark. K.S. was supported by a Rockefeller Foundation Fellowship.

F-AM-H9 ROLE OF TEMPLATE, SUBSTRATE AND METAL IN THE RESPONSE OF Qβ POLY (C) AND POLY(CU_2) POLYMERASE TO ORTHOPHOSPHATE AND PYROPHOSPHATE. Robert R. Brooks, O. Elmo Millner, Jr.* and Jon A. Andersen*, Norwich Pharmacal Co., Div. of Morton-Norwich Products, Inc., Norwich, New York, 13815.

Understanding the interaction between viral nucleic acid polymerases and the components of their synthetic complexes may hold the key to chemotherapy of viral pathologies. The Qβ bacteriophage enzyme, one model for this purpose, uses polycytidylate-uridylate (1:2) as template (Hori et al., Proc. Natl. Acad. Sci. 57:1790, 1967). We have characterized this reaction. It is dependent on both poly(CU_2) and substrates (ATP,GTP), and is linear with time from 0 to 20 min at 32°C and with protein at least up to 12 μg/ml. In accord with its composition, poly(CU_2) supports only 1/3rd the GMP incorporation as does poly(C). Both Mn^{++} and Mg^{++} satisfy the metal requirement with optima of 2-4 and 10-30 mM, respectively. Double reciprocal plots for poly(CU_2) give V_{max}'s of 1.33 and 0.30 nmoles/20 min and apparent K_m's of 46 and 31 μM (as nucleotide of template) for the Mn^{++} and Mg^{++} reactions, respectively. Template and metal mediate sensitivity to phosphorylated inhibitors. Thus the poly(CU_2) reaction is more sensitive to $P_2O_7^{-3}$ than the poly(C) system. The opposite holds for PO_4^{-2}. Reactions run with Mn^{++} are up to 100-fold more sensitive to these compounds than those run with Mg^{++}. Experiments in which enzyme and compound are incubated with various components of the reaction mixture indicate that, in general, both GTP and template protect the enzyme from inhibition. The effect of Mn^{++} is more complex. For example, it protects the poly(C) reaction from both PO_4^{-2} and $P_2O_7^{-3}$, but sensitizes the poly(CU_2) system to $P_2O_7^{-3}$.

F-AM-H10 REPLICATION OF MYCOPLASMAVIRUS SINGLE-STRANDED CIRCULAR DNA. J. Maniloff and J. Das*, Depts. of Microbiology and of Radiation Biology and Biophysics, Univ. of Rochester, Rochester, N.Y. 14642.

Replication of mycoplasmavirus single-stranded circular DNA has been shown to involve three replicative intermediates: the parental chromosome is converted to closed circular double-stranded DNA (RFI); RFI is nicked to give a relaxed double-stranded circular DNA (RFII); from RFII single-stranded circular DNA progeny chromosomes (SSI) are produced, and SSI becomes associated with viral proteins to form a partially packaged chromosome (SSII). SSII is the form of the progeny DNA which is extruded through the mycoplasma cell membrane without lysing or killing the cell. The effect of rifampicin (rif) and chloramphenicol (cam) on virus replication has been studied using rif resistant Acholeplasma laidlawii host cells. Rif only partially inhibits virus production if added early in infection, but if added late in infection, complete inhibition is found. Possible explanations for this time dependence will be discussed. Since the cells' RNA polymerase is rif resistant, the RNA polymerase involved in viral replication must be somehow different to make it rif sensitive. Cam inhibits virus production at all infection times. The effects of the antibiotics on the viral DNA replicative intermediates will be discussed.

F-AM-H11 EVIDENCE FOR AN INDUCIBLE ERROR PRONE REPAIR SYSTEM IN ESCHERICHIA COLI B. S. G. Sedgwick* (Intro. by A. Hollaender), Biology Department, Brookhaven National Laboratory, Upton, New York 11973.

A current hypothesis is that UV induced mutagenesis arises from the induction of an error prone mode of postreplication repair that requires the exr^+ $recA^+$ genotype (1). This hypothesis was tested using alkaline sucrose gradient centrifugation coupled with assays of mutation fixation determined by loss of photoreversibility. It was found that the protein synthesis inhibitor chloramphenicol added before irradiation prevented a small amount of postreplication repair and completely eliminated mutation fixation in E. coli WP2s uvrA. However, chloramphenicol did not affect strand joining: a) in uvrA bacteria allowed 20 min growth between irradiation and antibiotic treatment; b) in nonmutable uvrA exrA bacteria; and c) in uvrA tim bacteria grown at 42° C for 70 min before irradiation (tim is a nonfilament inducing derivative of tif (1) and causes elevated mutability at 42° C). These observations indicate that an inducible product is involved in postreplication repair and is responsible for induced mutagenesis. This research was carried out at Oak Ridge National Laboratory under contract with the Union Carbide Corporation and at Brookhaven National Laboratory both sponsored by the U. S. Atomic Energy Commission.

(1) Witkin, E. M., 1974, Proc. Nat. Acad. Sci. USA 71: 1930-1934.

F-AM-H12 MOLECULAR THEORY OF DNA POLYMERASE-DEPENDENT MUTAGENESIS* D.J. Galas* and E.W. Branscomb*, Biomedical Division, Lawrence Livermore Laboratory, University of California, Livermore, California 94550.

Mutations in the gene coding for the DNA polymerase of the bacteriophage T4, which confer mutator or antimutator phenotypes, provide the basis for investigations into the molecular mechanisms of the mutagenic action of this gene product. We have constructed a theoretical model of the action of the polymerase in inserting and excising bases during DNA replication. This simple sequential-stochastic model has been analytically solved. We are able to evaluate explicitly, for several mutant polymerases, (1) the frequency of multiple excisions of bases and the contribution this makes to accuracy, (2) the trade-off between polymerization speed and accuracy, and (3) the magnitudes of a number of parameters characterizing the random walk properties of the polymerase function. The theory also makes precise predictions for the dependence of these quantities (including all measured variables) on the relative and absolute concentrations of correct and incorrect substrate deoxynucleoside triphosphates. Application of the results to existing data from in vitro experiments** on a well studied set of mutant polymerases provides a simple interpretation of the enzymatic nature of the mutational change among the several mutator and antimutator polymerases.

The theory predicts the quantitative results of a number of suggested experiments, providing further tests of the validity of the explanations.

*This work was performed under the auspices of the U.S. Atomic Energy Commission.

**M.J. Bessman et al., J. Mol. Bio. (1974) 88, 409-421.

F-AM-H13 LACTOSE OPERON REPRESSOR INTERACTION WITH INDUCER AND DNA: CHANGES IN TRYPTOPHAN FLUORESCENCE.
Hans Sommer‡ Ponzy Lu, Department of Chemistry, University of Pennsylvania, Philadelphia, and Jeffrey Miller‡ Department of Molecular Biology, University of Geneva, Geneva, Switzerland.

The lactose operon repressor from E.coli, a tetrameric protein with two tryptophan residues per subunit, can bind specific DNA sequences and some disaccharides, i.e. inducers or anti-inducers. It is possible to follow the binding of inducer molecules to this protein by observing changes in the tryptophan fluorescence [Laiken, Gross, and von Hippel, J. Mol. Biol. (1972) 66, 143]. We have found that it is also possible to follow the interaction of the repressor molecule with DNA by observing tryptophan fluorescence changes. These results are in qualitative agreement with studies made by Millipore filter binding studies [Riggs, Lin, and Wells, Proc. Nat. Acad. Sci. (1972) 69, 761]. By using suppressed nonsense mutations at the two tryptophan positions, amino acids 190 and 209 respectively, it is possible to show which tryptophan is responsible for the fluorescence changes. The fluorescence change seen upon inducer binding arises from tryptophan 209 while both tryptophans contribute to the changes seen upon binding repressor to DNA. Some of the physical characteristics of the altered repressors molecules made by suppression of nonsense mutation at the two tryptophan sites will be described.

This work is supported by the American Cancer Society.

F-AM-H14 STRUCTURE-FUNCTION RELATIONSHIP OF LAC REPRESSOR FROM E. COLI.
P. Bandyopadhyay* and C.W. Wu, Department of Biophysics, Albert Einstein College of Medicine, Bronx, N. Y. 10461.

Chemical modifications of lac repressor were performed to determine the functional roles of various amino acid residues. It was possible to modify all three cysteine residues per monomer of the repressor using 5-5'-dithiobis (2 nitrobenzoic acid). The modified repressor was active with respect to inducer binding but lost the ability to bind lac operator. Lac repressor was covalently labeled with a fluorescent analog of iodoacetamide, 1,5 I-AENS. The fluorescent-labeled repressor bound IPTG efficiently, and nanosecond fluorescence depolarization studies showed that there was no gross structural change of the repressor upon binding IPTG. Tetranitromethane modified five of the eight tyrosine residues per monomer of the repressor. The nitrotyrosine repressor was still active in inducer binding. The nitrotyrosine was reduced to aminotyrosine and subsequently reacted with dansyl chloride. No fluorescence change was detected when IPTG was added to the dansylated repressor indicating that the environment of most of the tetranitromethane accessible tyrosine residues did not undergo significant alteration. One tyrosine and one or two histidine residues per monomer of lac repressor were modified using diazonium-1H-tetrazole. Such modified repressor had reduced inducer binding activity. Of particular interest is the iodination of one tyrosine residue per monomer by lactoperoxidase. Addition of IPTG to the iodinated repressor resulted in an enhancement of fluorescence intensity of iodotyrosine indicating a conformational change of the protein. A fluorescence change was also observed when lac operator fragments were added to the iodinated repressor. No such change was seen with non-specific DNA.

F-AM-I1 EFFECT OF SOME GENERAL ANESTHETICS ON WATER NEAR LIPID BILAYER SURFACES R.G. Parrish and R.J. Kurland, Department of Chemistry and Ross Markello*, Department of Anesthesiology, School of Medicine, SUNY at Buffalo Buffalo, New York.

General anesthetics are widely used in surgical procedures, yet little is known about the mechanism by which they induce narcosis. Theories proposed to explain the phenomenon fall into two categories: 1) a membrane site of action and 2) an aqueous site of action. Evidence has accumulated recently which demonstrates that anesthetic agents do indeed perturb not only the lipid bilayers but also the activity of proteins located within the bilayers. Experiments designed to determine the action of anesthetics at approximately physiological conditions on water near cell membranes have not, to our knowledge, been reported. We have measured nuclear magnetic resonance relaxation rates of protons and sodium in membrane systems. The increase in proton relaxation rates with increasing anesthetic concentration suggests that one effect of the anesthetic is to produce motional restriction in water molecules, either in the bulk phase or near membranes. Additional studies have shown a similar increase in relaxation rate with increasing anesthetic concentration occurs in the absence of membranes when solutes known to "order" water are also present.

F-AM-I2 THE EFFECTS OF PLASTOQUINONES ON THE PHOTOCONDUCTIVITY AND PHOTOVOLTAGE OF CHLOROPHYLL a CONTAINING LIPID BILAYERS: COUPLING OF PHOTONS, PROTONS AND ELECTRONS. Barry R. Masters* and David Mauzerall. The Rockefeller University, New York, New York 10021

A planar lipid bilayer formed from egg lecithin in n-decane and doped with Chl a when separating asymmetric solutions of reductant and oxidant, is capable of developing both a photopotential and a photoconductivity when exposed to continuous light from a Helium-Neon laser. The light beam is focused down to illuminate only the thin portion of the BLM. The photoresponse varies directly with the area illuminated. The photoconductivity of Chl a BLM is independent of light intensity, but the photopotential is linear with intensity over the range employed. The method of Hong and Mauzerall (BBA 275, 479-484, (1972) is employed to separate the photoconductivity and the photopotential under voltage clamp conditions. The incorporation of plastoquinones (PQ-5 or PQ-9) into the BLM acts as a shuttle for electrons between the two interfaces. This leads to an increase in the dark conductance in the presence of PQ-5 by an order of magnitude. Typical results: Chl a 3.5 mM, PQ-5 20 mM, 0.1 N KCl, 10 mM ferricyanide, 10 mM ferrocyanide. Dark conductance: egg lecithin 0.007 nmhos, +Chl a 0.1 nmhos, +PQ-5 1.6 nmhos. The light conductance is 1.6 nmhos. In the presence of Chl a + PQ-5 the dark voltage is 4 mV, and the value is 10 mV in the light. The effects of various quinones, oxidents, reductants and pH gradients on the photoconductance and the photopotential were studied. These studies are one step in the partial reconstitution of the photosynthetic unit.

F-AM-I3 Effect of Calcium Ions on Rectification Phenomenon of Lipid Bilayer Membranes. S. Ohki and R. Sauve*, Department of Biophysical Sciences, State University of New York at Buffalo, New York 14226

Rectification phenomenon was observed for an acidic phospholipid (phosphatidyl-serine) bilayer membrane when a bi-ionic (K^+ and Na^+) condition was set up across the membrane. This rectification was enhanced by the addition of a small amount of calcium ions on Na^+ side. The response potential behavior for the application of a brief constant current was similar to those observed for the squid axon membrane with subthreshold currents. The degree of rectification was a function of calcium concentration on one side. The mechanism of rectification due to the bi-ionic condition is analyzed in terms of the difference in ionic permeabilities between K^+ and Na^+, as well as the membrane surface potential, and the enhancement of the rectification due to the addition of calcium ions on one side of the membrane is partly explained by the calcium adsorption on the membrane surface. (this work was partly supported by NIH grant 2R01 NS 08739)

F-AM-I4 AN ATP-SODIUM PSEUDO PUMP. Edward S. Hyman, Touro Research Institute, New Orleans, Louisiana 70115

In the controls for a study of solubilized ATP-ase incorporated into a sphingomyelin-cardiolipin membrane, dilute Na_2 ATP was observed to affect the phospholipid membrane without enzyme. In a cell containing 0.1 M NaCl on both sides of a "not black" membrane, addition of as little as 0.001 N Na_2 ATP to the cis-side caused the open circuit voltage (OCV) on that side to become 90 to 110 MV negative to the trans-side. The "short circuit current" (SCC) was in the direction of pumping Na against a gradient. It rapidly peaked at 5 x 10^{-7} A/cm^2 and decayed in 15 minutes. With 0.01 N Na_2SO_4 in cis-chamber and 0.1 N in the trans-chamber making the cis-chamber positive, addition of 0.001 N Na_2 ATP causes an equal change in OCV and SCC, each of which crosses zero. Di isooctyl phosphate can be substituted for cardiolipin in the phospholipid membrane. The phenomenon is reproducible in a not black or in a black cardiolipin-decane membrane. The OCV and SCC are less with phosphatidylserine > phosphatidylethanolamine >> lecithin and not obtained with sphingomyelin. Using cardiolipin the change in OCV and SCC is obtained with $Na_3P_5O_{10}$ and sodium cellulose polysulfate, less so with Na_2 ADP, and minimally with Na3 citrate and Na benzene sulfonate. The direction is reversed with the Na salt of the more lipid soluble anion dodecyl benzene sulfonate. No change is observed with 0.001 N Na_2SO_4. The magnitude of the OCV greatly exceeds the Donnan potential. The large SCC is not due to hydrolysis of ATP but is likely due to charging of a capacitor with about 1 Na/7Å^2 of membrane. The phenomenon is not only an important control for the study of ATP-ase, but since cardiolipin is contained in solubilized ATP-ase, it suggests a means of alignment of ATP in the enzyme at least in part by way of its counter-ions.

Supported by NIH Grant

F-AM-I5 A FULLY ACTIVE AND HIGHLY FLUORESCENT ANALOG OF GRAMICIDIN A: SIMULTANEOUS CONDUCTANCE AND FLUORESCENCE MEASUREMENTS ON PLANAR LIPID BILAYER MEMBRANES. W. R. Veatch*, R. Mathies*, M. Eisenberg*, and L. Stryer, Department of Molecular Biophysics and Biochemistry, Yale University, New Haven, Connecticut 06520.

Gramicidin A is a linear polypeptide antibiotic that allows alkali cations and hydrogen ions to traverse lipid bilayer membranes. There is much evidence that gramicidin forms a polar channel spanning the hydrophobic membrane interior. It has been proposed that the channel is a conducting dimer in equilibrium with non-conducting monomers in the membrane. The most direct test of this model requires that the amount of gramicidin in the membrane be directly measured. O-dansyltyrosine gramicidin C is an analog of gramicidin A with fluorescence emission maximum near 540 nm and a quantum yield on membranes of 0.6. The kinetic and equilibrium conductance parameters of O-dansyltyrosine gramicidin C are very similar to those of gramicidin A. For a thick membrane (in which nearly all of the gramicidin is monomeric), a plot of the logarithm of membrane conductance versus the logarithm of the membrane fluorescence has a slope of approximately two, which demonstrates that the channels are indeed dimers. The gramicidin dimerization constant was found to be strongly dependent upon lipid structure as well as upon membrane thickness. Our measurements of the channel and total gramicidin surface densities for a thin membrane reveal that most of the gramicidin is in the conducting dimer state. Thus, it will be feasible to carry out spectroscopic studies of the conformation of the transmembrane channel. Supported by a grant from the National Institute of General Medical Sciences (GM16708).

F-AM-I6 BLOCKING OF VALINOMYCIN-K^+ CONDUCTANCE IN LIPID BILAYER MEMBRANES BY A SERIES OF BENZIMIDAZOLES. K.-H. Kuo* and L. J. Bruner, Department of Physics, University of California, Riverside, CA 92502.

The following series of substituted benzimidazoles have been tested for their ability to block Val-K^+ conductance in PE bilayers:

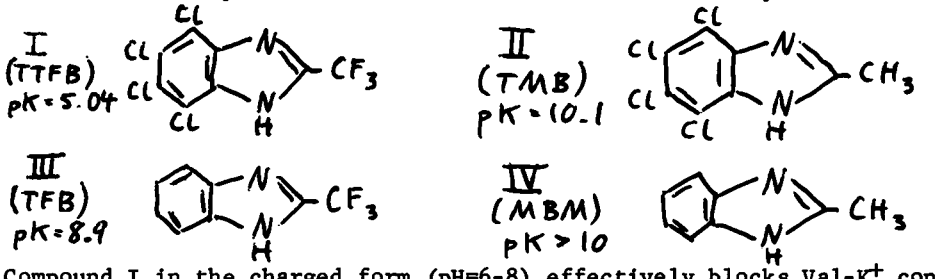

Compound I in the charged form (pH=6-8) effectively blocks Val-K^+ conductance, as previously reported.[1] Compound II, though neutral in the same pH range, also blocks Val-K^+ conductance at concentrations of 10^{-5}M and higher. Compounds III and IV are ineffective as blocking agents. We conclude that: a) Halogenation of the aromatic ring is essential to the blocking effect, b) Blocking is enhanced if, in addition, the compound is negatively charged, with pH > pK. Compound II permits the most detailed study of blocking, since it makes no direct contribution to bilayer conductance. In this case a transition from superlinear to sublinear I-V curves is noted at the onset of blocking, suggesting that II acts by inhibiting Val-K^+ complexation or dissociation at the membrane surface. This work is supported by the U.S. Army Research Office.

1. Biochem. Biophys. Res. Commun. 52, 1079, (1973).

F-AM-I7 THE UTILITY OF THE STERN EQUATION IN DESCRIBING THE ADSORPTION OF CHARGED MOLECULES TO BILAYER MEMBRANES. Stuart McLaughlin and Howard Harary, Dept. Physiology and Biophysics, SUNY, Stony Brook, N.Y., 11794.

To describe quantitatively the adsorption of charged amphipathic molecules (e.g. the salicylates, local anesthetics, biguanides; certain fluorescent probes, pH indicators and uncouplers of oxidative phosphorylation) to biological and bilayer membranes, one must recognize that the adsorption of the charged molecules produces an electrostatic potential at the membrane solution interface, which can be described most simply by the Gouy equation from the theory of the diffuse double layer. This surface potential will tend to lower the concentration of the adsorbing ions in the aqueous phase immediately adjacent to the membrane, a phenomenon which can be described by the Boltzmann relation. The number of adsorbed ions is, in turn, a function of the aqueous concentration of these ions at the membrane solution interface, and can be described, in the simplest case, by a Langmuir adsorption isotherm. The Stern equation, a combination of the Gouy, Boltzmann and Langmuir relations, was found to be capable of describing in a self consistent manner some existing data obtained with amphipathic molecules at different concentrations of indifferent electrolyte. Direct, accurate measurements of the number of moles of TNS bound to phospholipid vesicles are also available (Huang & Charlton, Biochemistry, 1972, 11, 735). A computer program is described which provides a best fit of the Stern equation to such data. Although the curves generated by the Stern equation closely resemble linear Scatchard plots, the values of the association constants and number of binding sites differ significantly. Experimental evidence is presented that TNS does in fact change the surface potential of bilayers. Supported by NIH grant NS10485.

F-AM-I8 LOCATION OF CATIONS COMPLEXED BY NEUTRAL CARRIERS IN LIPID BILAYER MEMBRANES. Gabor Szabo. Department of Physiology, University of California, Los Angeles, California 90024.

Cationic (steady-state Na^+ and instantaneous NH_4^+) conductances induced in monoolein-cholesterol-decane bilayers by the neutral carriers, nonactin, trinactin and valinomycin were found to be depressed equally (45 fold for a cholesterol/monoolein mole fraction, x = .75) by increasing cholesterol content of the lipids. For small cholesterol mole fractions ($x \leq .75$) virtually all of this conductance decrease could be attributed to the effect of an increasingly positive electrostatic potential which results from altered surface dipoles by cholesterol and whose magnitude has been previously assessed by the use of lipophilic cations and anions (Szabo, Nature 252:47, 1974). In order to determine whether the rate of translocation, k_{is}, or the formation constant, K_{is}, of the ion-carrier complex is altered by the surface-dipole induced electrostatic potential, kinetic parameters of transport were measured for the NH_4^+-trinactin system. The results indicate that the major effect of the dipole potential is to decrease the rate of translocation ($k_{is} \simeq 5 \times 10^3$ for x = 0; $k_{is} \simeq 1 \times 10^3$ for x = 0.5), without altering significantly the formation constant of the charged complex or the concentration of the membrane-bound neutral carrier. Assuming that the dipole potential originates in the region of the polar head groups, one must conclude that the ion-carrier complex is adsorbed, and presumably formed, at the aqueous side of the lipid polar head groups since otherwise K_{is}, not k_{is}, should decrease. Cationic complexes of neutral carriers appear to resemble lipophilic ions (e.g. tetrephenylborate) in that they adsorb at the membrane surface in a similar environment. Supported by Grants from MDAA and NIH (GB 30835).

F-AM-I9 POTENTIAL ENERGY BARRIERS TO ION TRANSPORT WITHIN LIPID BILAYERS: STUDIES WITH TETRAPHENYLBORATE. By Olaf Sparre Andersen* and Martin Fuchs* (introduced by E.E. Windhager). Dept. of Physiology and Biophysics, Cornell University Medical College, New York, N.Y. 10021.

Tetraphenylborate ($TPhB^-$) current transients were studied in lipid bilayers formed from bacterial phosphatidyl ethanolamine in decane. Ion movement was essentially confined to the membrane interior during the current transients. Charge movement through the interior of the membrane during the current transients was studied as a function of the applied potential. As expected, the transferred charge approached an upper limit with increasing potential, which is interpreted to be the amount of charge due to $TPhB^-$ ions absorbed into the boundary phase of the bilayer. A further analysis of the charge transfer as a function of potential indicates that the movement of $TPhB^-$ ions is only influenced by 75% of the applied potential. The initial conductance and the time constant of the current transients were studied as a function of potential. It was found that an image-force potential energy barrier gave good prediction of the observed behavior, provided that the effective potential was used in the calculations. We could not get a satisfactory prediction of the observed behavior with an Eyring rate theory model or a trapezoidal potential energy barrier. We conclude that an analysis of the potential energy barrier to ion transport in the middle of the membrane is dependent on a model-independent determination of the effective potential observed by the current carrier. Supported by NIH Grant #GM 21342.

F-AM-I10 CAN ELECTRON CONDUCTION OCCUR ACROSS BILAYER LIPID MEMBRANES?# Paul Shieh and H. Ti Tien, Department of Biophysics, Michigan State University, East Lansing, Mich. 48824.

In 1957, Arnold and Sherwood [PNAS, 43, 105] posed the question "Are chloroplasts semiconductors?" and promptly supplied an affirmative answer. Over the years the work of many investigators has led to a "solid-state" theory of photosynthesis, in which the thylakoid membrane plays the crucial role. However, direct physical chemical characterization of the thylakoid membrane has been difficult owing to the complexity of the system and lack of suitable technique for its isolation and study. One approach to mitigating these difficulties has been to investigate model membrane systems such as the bilayer lipid membrane (BLM). As have been found by many workers, pigmented BLM exhibit interesting photoelectric effects and possess certain properties characteristic of semiconductors.

The present paper is concerned with electronic processes in non-pigmented BLM in the absence of light. Such processes, termed electrostenolysis, which have been known in other membrane systems, will be briefly reviewed. In addition, experimental evidence in support of electrostenolysis in BLM will be presented.

#For a detailed discussion on this question, see Bilayer Lipid Membranes (BLM): Theory & Practice, Marcel Dekker, Inc., New York, 1974, pp. 217-244 and Chapter 9.

(Supported by College of Osteopathy MSU and USPHS grant GM-14971)

F-AM-I11 EFFECT OF PHLORETIN ON CONDUCTANCE OF LIPID BILAYERS. H.P. Ting-Beall, Dale J. Benos, James E. Hall & D.C. Tosteson: Dept. Physiology & Pharmacology, Duke University Medical Center, Durham, N.C. 27710.

We have measured the effect of phloretin(10^{-4}M) on the steady state voltage(V)-current(I) curves of bilayers(sheep red cells or lecithin) exposed to various conductance increasing substances:valinomycin, PV, nonactin, $(C_6H_5)_4As^+$, and alamethicin. In all experiments(except ala) 1M KCl bathed both sides of the membrane and T= 23°C. For all the substances tested, the results were independent of pH(5-9, phloretin pK = 7·2), but differed markedly from substance to substance. For val, addition of phloretin to one side decreased the current flowing toward that side. Bilateral phloretin decreased current in both directions and changed the I-V curve from saturating to superlinear up to 150mV. There was zero-current potential (V_m^o). For PV, unilateral phloretin produced a V_m^o of 50 to 70 mV. Bilateral phloretin changed the I-V curve from saturating to superlinear, and abolished V_m^o. For non, addition of phloretin to one side increased preferentially the current flowing away from that side but also increased current flowing toward that side. Bilateral phloretin increased the current in both directions and changed the I-V curve from superlinear to saturating. For 10^{-3}M $(C_6H_5)_4As^+$, addition of phloretin to one side increased current symmetrically by two orders at all voltages, and the I-V curve remained superlinear. For 10^{-6} g/ml ala (0·01 M KCl), addition of phloretin to one side increased symmetrically by 20mV the voltage at which G_m began to increase exponentially. From these results we conclude that phloretin can alter both reaction rates between K^+ and carrier at the membrane surface asymmetrically and the energy required for translocation of charged species.

(Supported by NIH Grant HL-12157)

F-AM-I12 ION TRANSFER ACROSS THIN LIPID FILMS IN THE PRESENCE OF HEMOCYANIN. R. Latorre*, O. Alvarez* and E. Diaz*, Laboratory of Biophysics, IR, NINDS, National Institutes of Health, Bethesda, Md. 20014 and Departamento de Biologia, Facultad de Ciencias, Universidad de Chile, Santiago, Chile. (Intr. by Robert E. Taylor).

When hemocyanin, the characteristic blood pigment of many invertebrates, is added to a black lipid film the conductance increases in discrete steps. For negative potentials the step conductance is constant. In 0.1 M KCl the step conductance is 2×10^{-10} mho. For positive potentials the step conductance appears to decrease as the potential increases. At high positive potentials the conductance fluctuates between several levels. The data suggest that hemocyanin conducts ions through discrete channels. The channel shows a very low anion permeability and the channel conductance approaches a limiting value at high electrolyte concentrations. The voltage dependent conductance observed when large amounts of hemocyanin are added to the membrane seems to be the consequence of the properties of the single hemocyanin channel.

F-AM-113 THE EFFECT OF PENTACHLOROPHENOL ON ELECTRICAL CONDUCTIVITY OF LIPID BILAYERS. Kwan Hsu and Pavel Smejtek*, Department of Physics, Portland State University, Portland, Oregon 97207

Black membranes formed from lipids, cholesterol and decane were used as models to investigate one of the possible mechanisms by which pentachlorophenol (PCP) can alter properties of biological membranes. DC conductivity characteristics of membrane containing either phosphatidylcholine or phosphatidylethanolamine were measured as a function of pH of the bathing medium and PCP concentration. The conductivity versus pH curve exhibits a maximum at different values of pH for different lipids, but the position is independent of PCP concentration. At low PCP concentrations (10^{-6}-10^{-5} M/L) the membrane conductivity in the region of conductivity maximum is a quadratic function of the PCP concentration, but on the alkaline side it becomes linear. Measurements made with nonactin-potassium probe indicate strong adsorption of PCP molecules on the membrane surface. The experimental results are consistent with the hypothesis that the increase of membrane conductivity in presence of PCP is due to negatively charged complex formed by ionized and neutral molecules.

Supported by NIH grant ES 937.

F-AM-J1 CATION FLUX IN THE EHRLICH ASCITES TUMOR CELL. Barry Mills* and Joseph T. Tupper. Department of Biology, Syracuse University, Syracuse, New York 13210. (Intr. by Erich Harth).

The components of unidirectional Na and K flux have been investigated in the Ehrlich ascites tumor cell. The data are consistent with the presence of a component of K efflux dependent on the presence of external K. The magnitude of the K dependent K efflux is maximal at approximately 50 mM intracellular K and it represents 48% of the total efflux. The K dependent efflux is not saturable since it diminishes upon further elevation of intracellular K. At 100 mM intracellular K it represents 22% of the total efflux. The results also show the presence of a component of Na efflux dependent on the presence of external Na. The Na dependent component of Na efflux represents 57% of the ouabain insensitive Na efflux and 31% of the total Na efflux at 147 mM external Na. Upon reduction of extracellular Na, the Na dependent component diminishes with an apparent K_m for external Na of 10 mM. Evidence will be presented that the K dependent K efflux and the Na dependent Na efflux represent one for one K-K and Na-Na exchange mechanisms. By subtraction of the ouabain sensitive component and the Na dependent component of Na efflux from the total unidirectional Na efflux and by subtraction of the K dependent component from the total unidirectional K efflux, the magnitude of the diffusional components of Na and K efflux have been estimated. From these, the permeabilities to Na and K have been determined. These permeabilities yield a value for cell membrane potential of -18 mV. This is in good agreement with the -21 mV predicted from ^{36}Cl distribution. Supported by grants from the American Cancer Society (BC-181) and the Syracuse University Research Fund.

F-AM-J2 FUROSEMIDE SENSITIVE Na AND K FLUX IN THE EHRLICH ASCITES TUMOR CELL. Joseph T. Tupper, Department of Biology, Syracuse University, Syracuse, New York 13210.

Furosemide inhibits components of Na and K unidirectional flux in the Ehrlich ascites cell. These components are distinct from the ouabain sensitive components of Na efflux and K influx. Unidirectional K influx is inhibited 29% by 10^{-3}M furosemide, a concentration at which its effect is maximal. Unidirectional K efflux is inhibited 34% by 10^{-3}M furosemide. Removal of external K reduces the inhibition of K efflux to approximately 11%. Unidirectional Na efflux is reduced 24% by 10^{-3}M furosemide. Cells exposed to furosemide do not gain Na or lose K, as compared to control cells. In the presence of ouabain cells from the same population gain Na and lose K. Cells were depleted of K and loaded with Na by incubation in the cold. Furosemide does not prevent these cells from regaining K and expelling Na upon warming whereas this is completely abolished by ouabain. The data indicate that furosemide alters unidirectional but not net Na and K fluxes. This is consistent with the conclusion that the furosemide sensitive fluxes represent one for one Na-Na and K-K exchange mechanisms. Furthermore, the magnitudes of these components are in reasonable agreement with the magnitudes of an external Na dependent Na efflux and an external K dependent K efflux previously identified in this cell line (Mills and Tupper, these abstracts). Supported by grants from the American Cancer Society (BC-181) and the Syracuse University Research Fund.

F-AM-J3 THE ENERGETIC BASIS OF AMINO ACID TRANSPORT INTO S37 ASCITES TUMOR CELLS. R. H. Matthews and M. Sardovia*, Department of Physiological Chemistry, The Ohio State University, Columbus, Ohio 43210.

Energy-requiring accumulation of amino acids appears to occur in several mammalian tissues, including intestine, kidney, and ascites tumor cells. Transport is inhibited by a variety of metabolic inhibitors. The direct energetic basis for amino acid transport has, however, been a subject for debate. Two possibilities which have been put forward but rejected as inadequate are that ATP itself supports transport directly, and that amino acids are cotransported with sodium so that the sodium gradient can be the immediate energetic basis for concentrative amino acid transport. Meister and coworkers have proposed a cycle of reactions involving the breakdown and synthesis of glutathione as the basis for amino acid transport in brain and kidney. We find that the γ-glutamyl cycle is the principal energetic basis for two amino acid transport systems of the S37 ascites tumor cell, which are known as the A and L systems. These transport systems have been studied functionally in several laboratories. One is stimulated much moreso than the other by sodium; the second is a much better exchange system than the first. There are several items of evidence for the involvement of the γ-glutamyl cycle in amino acid transport into S37 ascites tumor cells. Dihydro orotic acid, which inhibits 5-oxoprolinase, inhibits amino acid transport; orotic acid does not. L-methionine-S-sulfoximine, which inhibits γ-glutamyl cysteine synthetase, also inhibits amino acid transport. Glutathione itself is mildly inhibitory to amino acid transport when extracellular, but it is capable of reversing cyanide-induced inhibition of amino acid transport when present intracellularly.

F-AM-J4 CALCIUM FLUXES IN INTERNALLY-DIALYZED GIANT BARNACLE MUSCLE FIBERS, J. M. Russell and M. P. Blaustein, Department of Physiology and Biophysics, Washington University School of Medicine, St. Louis, MO 63110

Calcium-45 fluxes have been measured in isolated barnacle muscle fibers bathed in standard artificial seawater and subjected to internal solute control by means of internal dialysis with a solution containing Ca-EGTA buffers. The 45-Ca efflux was dependent upon the concentrations of both total and ionized Ca. With a constant total Ca of 2.0 mM the Ca efflux saturated as the nominal ionized Ca concentration ($[Ca^{2+}]i$) was increased from 0.032 to 0.52μM; the efflux was half saturated at $[Ca^{2+}]i \simeq 0.10\mu M$. However, when $[Ca^{2+}]i$ was maintained at 0.13μM (Ca:EGTA=1:2) and total Ca was reduced from 2.0 to 0.058 mM, 45-Ca efflux fell from 1.2 to 0.06 pmole/cm^2·sec. Ca efflux did not appear to be a buffer leak because with a 2.0:2.5 Ca:EDTA ratio (Mg-free, $[Ca^{2+}]i \simeq 0.13\mu M$), 45-Ca efflux was 2.35 pmole/cm^2·sec and 14-C-EDTA efflux was only 0.09 pmole/cm^2·sec., although the EDTA efflux may be underestimated because of the convoluted surface morphology. 45-Ca influx was 0.36 pmole/cm^2·sec in fibers dialyzed with 2.0 mM Ca-4.0 mM EGTA ($[Ca^{2+}]i = 0.13\mu M$). The influx was unaffected by CN(2 mM), oligomycin (25μg/ml) or caffeine (2 mM). An unexplained and unexpected observation was that the 45-Ca influx rose to a steady level much more rapidly than did 45-Ca efflux.

F-AM-J5 EFFECT OF OSMOLARITY ON GLUCOSE UPTAKE IN SOLEUS MUSCLE
I.H. Chaudry, G.J. Planer*, M.M. Sayeed and A.E. Baue*, Department of Surgery, Washington University School of Medicine and The Jewish Hospital of St. Louis, St. Louis, Mo. 63110

The effect of hyperosmolarity on glucose uptake was studied in the presence and absence of insulin. Glucose uptake by isolated rat soleus muscle was measured by incubating the muscles for 1 hr at 37 C in a Tris-HCl buffer, pH 7.4, containing 10mM glucose and varying amounts of sorbitol to give the required osmolarity. The results, expressed in μmoles/g/hr, are mean of 8 determinations in each group, and indicate that under basal conditions, glucose uptake increased with the increase in medium osmolarity. However, in the presence of 0.1U/ml insulin, uptake reached optimum at physiological osmolarity, i.e. at 300 milliosmoles (mOs). Further increase in osmolarity resulted in a progressive decrease in glucose uptake in the presence of insulin, indicating insulin resistance at higher osmolarity. At 400mOs, glucose uptake in the absence and presence of 0.1U/ml insulin was the same. For insulin to produce its optimal stimulatory effect at 400mOs, 0.25U/ml insulin was required, which is 250 times the concentration of insulin required to produce its maximal effect at physiological osmolarity. Thus, normal osmolarity is needed for optimal insulin effect on glucose uptake.

Osmolarity (mOs)	Basal uptake	Insulin (U/ml)	Uptake with Insulin
180	14.6 ± 0.8	0.1	23.5 ± 1.0
240	15.3 ± 0.7	0.1	30.2 ± 0.9
300	17.8 ± 0.6	0.1	35.5 ± 1.2
360	19.3 ± 1.2	0.1	28.0 ± 1.1
400	26.2 ± 1.2	0.1	25.8 ± 0.9
400		0.25	35.3 ± 1.1

F-AM-J6 NUCLEAR AND CYTOPLASMIC POTASSIUM OF THE AMPHIBIAN OOCYTE.
M. Frank and S.B. Horowitz, Department of Biology, Michigan Cancer Foundation, Detroit, Michigan, 48201.

Potassium exchange in the mature amphibian oocyte, its nucleus and cytoplasm have been determined by ultra-low temperature microdissection. Oocytic K^+ consists of two distinct kinetic fractions, with the proportion of the slower fraction increasing with oocyte size. The rapidly exchanging fraction, $t_{\frac{1}{2}} \simeq 7$ hrs, accounts for 13-28% of the cellular K^+. It appears to occur in nucleus and cytoplasm in the ratio of about 1.8:1. This asymmetry is not membrane mediated. The slowly exchanging fraction, $t_{\frac{1}{2}} \simeq 2.3$ days, accounts for all of the remaining cellular K^+ and is limited to the cytoplasm, being bound or sequestered by an unidentified cytoplasmic component.

Nuclear and cytoplasmic K^+ concentrations are 120 mEq/L and 88 mEq/L H_2O respectively, in good agreement with determinations of Century et al. (J. Cell Sci. 7: 5, 1970). Hence an apparent paradox exists in that solute concentrations are lower in the "binding" phase (cytoplasm) than in the nonbinding phase (nucleus). Furthermore, electrometric measurements in similar oocytes (Dick and McLaughlin, J. Physiol. 205: 61, 1969) show activity coefficients for cytoplasmic K^+ similar to those of free solution. These paradoxes are resolved when the solute excluding properties of cytoplasm are considered.

Supported by National Science Foundation grant GB #27981, National Institute of Health grant GM #19548, and an institutional grant from the United Foundation of Greater Detroit.

F-AM-J7 ROLE OF THE ADP-SENSITIVE PHOSPHO-ENZYME IN THE REACTION CYCLE OF $(Na^+ + K^+)$-ATPase. C. Hegyvary, Department of Physiology, Rush Medical College, Chicago, Illinois 60612.

The phosphorylated form of native $(Na^+ + K^+)$-ATPase is sensitive to splitting by K^+ (E_2-P), but it becomes sensitive to splitting by ADP (E_1-P) if the enzyme is poisoned with N-ethylmaleimide (NEM) or oligomycin (OL). 1 mole of E_1-P binds 1 mole of ouabain in the presence of Mg^{++} + Pi, or of $Na^+ + Mg^{++}$ + ATP and somewhat less ouabain in the presence of Mg^{++} alone. Though E_1-P is not split by low concentrations of K^+, K^+ still slows ouabain-binding to E_1-P as well as to E_2-P. Thus K^+ may enhance dephosphorylation and inhibit ouabain-binding at two separate sites. The native enzyme can be phosphorylated by Pi and this phospho-enzyme can react with ADP to synthesize ATP. Ouabain partly inhibits this ATP-synthesis. NEM or OL do not modify phosphorylation from Pi but they decrease the synthesis of ATP and the inhibition of this synthesis by ouabain. These findings argue against a mandatory precursor-product relationship between E_1-P and E_2-P. (Supported by U. S. PHS Grant No. 1 RO1 HI 16611 - 01 from NHLI, NIH.)

F-AM-J8 SODIUM-CALCIUM EXCHANGE AND CALCIUM-CALCIUM EXCHANGE IN INTERNALLY-DIALYZED SQUID AXONS. M. P. Blaustein and J. M. Russell, Departments of Physiology and Biophysics, Washington Univ. School of Medicine, St. Louis, Mo., 63110 and University of Texas Medical Branch, Galveston, Texas 77550.

The influx and efflux of calcium (as ^{45}Ca) and influx of sodium (as ^{24}Na) were studied in internally-dialyzed squid giant axons. The axons were poisoned with cyanide and ATP was omitted from the dialysis fluid. The internal ionized Ca^{2+} concentration ($[Ca^{2+}]_i$) was controled with Ca-EGTA buffers. With $[Ca^{2+}]_i \geq 0.47$ μM, ^{45}Ca efflux was largely dependent upon external Na and Ca. The Na_o-dependent Ca efflux into Ca-free media appeared to saturate as $[Ca^{2+}]_i$ was increased to 160 μM; the half-saturation concentration was about 8 μM Ca^{2+}. In two experiments ^{24}Na influx and ^{45}Ca efflux were measured simultaneously; when $[Ca^{2+}]_i$ was decreased from 160 μM to 0.47 or 0.23 μM, Na influx declined by about 6 pmoles/cm^2sec, and Ca efflux declined by about 2 pmoles/cm^2sec. This may indicate that Ca efflux is coupled to Na influx with a stoichiometry of 3 Na^+-to-1 Ca^{2+}. Ca efflux into Na-free media required the presence of both Ca and an alkali metal ion (but not Cs) in the external medium. Ca influx from Li-containing media was greatly reduced when $[Ca^{2+}]_i$ was decreased from 160 to 0.23 μM, or when external Li was replaced by choline. These data provide evidence for a Ca-Ca exchange mechanism which is activated by certain alkali metal ions. The observations are consistent with a mobile carrier mechanism which can exchange Ca^{2+} ions from the axoplasm for either 3 Na^+ ions, or one Ca^{2+} and an alkali metal ion (but not Cs) from the external medium. This mechanism may utilize energy from the Na electrochemical gradient to help extrude Ca against an electrochemical gradient.

F-AM-J9 DIFFERENCES IN AMINO ACID TRANSPORT BETWEEN MYELOBLASTIC AND ERYTHROBLASTIC LEUKEMIA CELLS. W.C. Wise, Department of Physiology, Medical University of South Carolina, Charleston, South Carolina 29401.

The transport of α-aminoisobutyric acid (AIB), N-Methyl-AIB (N-MAIB), L-Alanine (ALA), and N-Methyl-ALA (N-MALA) have been studied in a myeloblastic leukemia (Shay Chloroleukemia)(SCL), and an erythroblastic leukemia (EBL) of the Long-Evans rat. The final steady state distribution ratio (Na = 135 mEq/l) for the EBL and SCL was 3.69 to 17.12 for AIB, 6.73 to 17.5 for ALA, 2.61 to 13.65 for N-MAIB, and 3.61 to 15.2 for N-MALA. The Na-dependent (Na-dep) transport system which needs both the free amino and carboxyl groups has a flux greater in SCL than in EBL for AIB, but not for ALA. The Na-dep transport system which needs only a free carboxyl group has a flux higher for both ALA and AIB in the SCL than in the EBL. The Na-dep N-Methyl requiring system and the Na-independent system have a higher flux in the SCL than EBL. Even though these two cells are basically one call division from the stem cell, their membrane transport systems are quite different. (Supported by PHS Research Grant [NCI] #CA13529 and RCDA #K04-CA 70412).

F-AM-J10 EVIDENCE OF DIFFERENTIAL CONTROL SYSTEM IN RAT ADIPOCYTE FOR GLYCOLYTIC AND SHUNT OXIDATION OF GLUCOSE.
*Sakti Prasad Mukherjee and William S. Lynn, Depts. of Biochem. and Medicine, Duke University, Durham, N.C. 27710

We have extended our earlier suggestion that insulin stimulates glucose transport in rat adipocytes by causing oxidation of some transport-specific sulfhydryls. It was found that the glycolytic and shunt pathways of glucose oxidation in these cells respond differently to the same redox agents which control transport rates. Oxidants, e.g., H_2O_2, vitamin K_5 or insulin stimulate both pathways, but reductants, e.g., Cysteine, Glutathione or Dithiothritol (DTT) inhibit glycolysis but enhance the shunt pathway of glucose oxidation. Phosphorylation of membrane components by treatment of cells with low concentrations of ATP inhibits the stimulatory effects on the shunt and depresses the glycolytic basal rates. The latter effect is additive to that of DTT. Adenylate Cyclase activity in membrane preparations from cells pretreated with DTT or ATP was reduced and pretreatment with oxidants caused its stimulation. These data suggest that the glucose transport system is controlled by adipocyte components, probably enzymes, closely associated with the membranes, which are modified both by sulfhydryl oxido-reduction and phosphorylation and the subsequent pathways of glucose oxidation differentially depend upon the internal redox potential. Further evidence that adenyl cyclase activity is coupled to the same redox and phosphorylation modifications suggests an important physiological role of Cyclic AMP in these differential controls.

F-AM-J11 NMR STUDIES OF HISTIDINE J BINDING PROTEIN FROM SALMONELLA TYPHIMURIUM. D. E. Robertson and C. Ho, Department of Biophysics and Microbiology, University of Pittsburgh, Pittsburgh, Pennsylvania 15260.

The osmotic shock-releasable binding proteins from gram-negative bacteria are known to play an important role in the transport of some amino acids, sugars, and ions across the cytoplasmic membrane. The histidine J binding protein (His J) from Salmonella typhimurium has been shown by genetic and biochemical evidence to be an essential component of the histidine transport system. High-resolution proton nuclear magnetic resonance (NMR) spectroscopy has been used in this study to investigate the conformation of His J in solution and the nature of its conformational changes upon the binding of L-histidine. 250 MHz proton NMR spectra of His J have been obtained over a wide range of such experimental conditions as pH, temperature, protein concentration, and substrate concentration. In solutions of D_2O at pD 7.1, the NH protons in the interior of the protein are nonexchangeable at 4°C, but do exchange with ^2H at 50°C within 10 minutes. At pD 5.5, the isoelectric point, however, the NH protons remain unexchanged after 1 hour at 50°C. Furthermore, when L-histidine is added, the methyl resonance region exhibits a general broadening and at least one resonance shows an upfield shift. Likewise, addition of L-histidine causes the disappearance of one ring-current shifted methyl proton signal and in the aromatic resonance region two signals collapse into a single line at 2.3 ppm downfield from HDO. These spectral changes are evident at low substrate: protein ratios and indicate a conformational change in His J upon ligand binding. The implications of these spectral changes on the mode of action of the histidine binding protein in the transport of histidine will be discussed. (Supported by NIH Grants GM-18698 and RR-00292 and NSF Grant GB-37096X).

F-AM-J12 ION COMPLEXATION IN THE NACTINS--A RAMAN SPECTROSCOPIC INVESTIGATION. George D.J. Phillies*, Irvin M. Asher, Byung J. Kim*, and H. Eugene Stanley, Harvard-M.I.T. Program in Health Sciences and Technology, M.I.T., Cambridge Mass. 02139.

We here report Raman spectroscopic studies of the macrocyclic ionophorous antibiotics nonactin, monactin, dinactin, trinactin, and tetranactin in well-characterized environments. Comparison with model compounds allows detailed assignment of spectral lines, especially those of the ester carbonyl, ester C-O-C, and tetrahydrofuran ring group vibrations. Solution spectra of the uncomplexed nactins indicate the sensitivity of the ester carbonyl groups to solvent polarity and to hydrogen bond formation. Spectra of crystalline uncomplexed nonactin, monactin, and tetranactin form one family, while spectra of dinactin and trinactin form a second, reflecting two basic crystalline arrangements. Spectra of the complexes of nonactin with eight monovalent cations of different size and charge distribution indicate that the cation-nactin ester carbonyl interaction depends on electrostatic interaction energy (calculated from a point charge model) rather than on ionic radius. Raman polarization studies and work on the nactin-barium complexes are also discussed.

F-AM-J13 EQUILIBRIA AND POSSIBLE SIGNIFICANCE OF THE CONFORMATION AND VOLUME CHANGES OF GRAMICIDIN A. M.Derechin, SUNYAB, Buffalo, N.Y. 14214.

Gramicidin A (GA) in absolute ethanol was shown (Derechin, Hayashi and Jordan,Life Sci.1974,15,403) to undergo a conformational transition with volume change so that at high dilution it fails to sediment in the ultracentrifuge. The present report shows also the occurrence in various media of a pressure-dependent system with species of different refractivity. Normal sedimentation,refractivity and volume are shown when water or Na^+ are present. Both agents unfold and dimerize GA. This behavior suggests the occurrence of equilibria of monomers (M) and dimers (D), possibly both in folded (F) and unfolded (U) states, as suggested in Fig.1. These properties of GA may be relevant to its biological function since the conformational transition with volume change may represent the transformation of the chemical energy of the transition into the mechanical energy needed to effect cation transport through membranes as suggested in Fig.2, with ⬭ = folded GA, ⬭— = unfolded GA, ⊕ = Na^+ and ⊜ = $PO_4^=$.

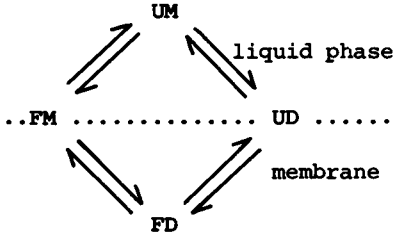

Fig.1

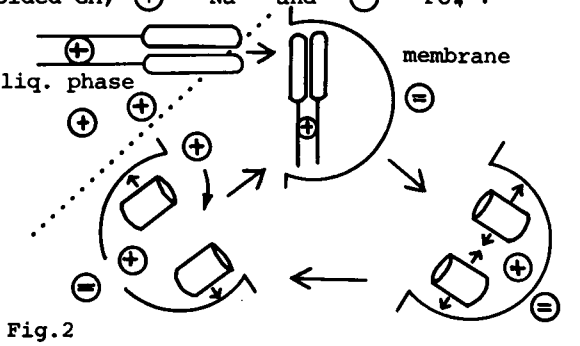

Fig.2

F-AM-K1 AN ELECTROMETRIC METHOD FOR RAPID MEASUREMENT OF CHLORIDE CONCENTRATION IN SMALL VOLUMES. M.A. Nunes,* K. Ogan, and A. Essig, Departments of Physiology, Instituto de Ciências Biomédicas, U.S.P., São Paulo, Brasil, and Boston University School of Medicine, Boston, Mass. 02118

Chloride concentrations was measured using the cell $Hg|Hg_2Cl_2|KCl_{(satd.)}$ ⁞salt bridge⁞ test solution|AgCl|Ag, and a high input impedance (10^{14} ohm) electrometer. The reference electrode was bridged to a micropipette of 15 μm tip diameter filled with 3M $NaNO_3$-agar. Silver wire of 10 μm tip diameter was shielded with epoxy-cement before chloridizing. Drops of less than 1 μl were placed on a glass silicone surface, covered with mineral oil, and probed with the aid of micropositioners. The EMF of the above cell was linear with the logarithm of chloride concentration in the range of 1 mM to 4 M, with a slope of 56 mV/decade (25°C). The system showed a drift of 2 mV after 24 hours. The response time of the system was less than 100 msec. Supported by Fundação de Amparo à Pesquisa do Estado de São Paulo-Brasil, and USPHS (Harvard-MIT Program in Health Sciences and Technology).

F-AM-K2 NOISE SPECTRUM DUE TO ENERGY FLUCTUATIONS FROM AN ELECTROLYTIC SOLUTION. M. Weissman* and G. Feher, Dept. of Physics, UCSD, La Jolla, CA.

The energy of a system fluctuates around its average energy by an amount $(\overline{\delta E^2}) = kTc$ giving rise to an effective temperature fluctuation $(\overline{\delta T^2}) = T^2k/c$ where k is Boltzmann's constant and c the specific heat. When a constant current is applied to a conducting system, the temperature dependence of the resistivity $\partial R/(R\partial T)$ produces a fluctuating voltage (1,2). We have measured the frequency spectrum in an electrolyte [saturated sol. of $ZnCl_2$ at 20°C, 18% glycerol (W/W), 0.03% HCl (W/W] with a large temperature coefficient (∿ -8%/degree). The experimental details were similar to those described earlier (1). The observed noise voltage V_N^2 minus the Johnson noise voltage V_J^2 is plotted logarithmically against f. Different frequency regions obey different power laws in approximate agreement with theory (2). Similarly, the integrated power spectrum agreed within ∿ 15% with the theoretically predicted value (2). At 40 Hz, $V_N^2/V_J^2 = 1.50$.

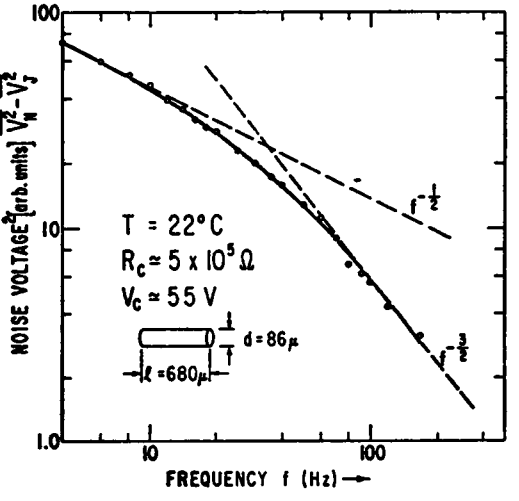

Work supported by NIH grant GM-13191.

(1) G. Feher and M. Weissman, P.N.A.S. (1973) 70, 870.
(2) J. Clarke and R. F. Vos, P.R.L. (1974) 33, 24.

F-AM-K3 SIMULATION OF ELECTRON PARAMAGNETIC RESONANCE SPECTRA PERTURBED BY SPIN-SPIN INTERACTIONS. K. L. Schepler*, W. R. Dunham* and R. H. Sands, Biophysics Research Division, Institute of Science and Technology, University of Michigan, Ann Arbor, Michigan 48105.

Several examples of weak electron spin-spin interactions have recently been observed in biological systems by electron paramagnetic resonance (EPR) spectroscopy. Computer programs have been written to calculate EPR powder spectra in cases where either isotropic exchange or dipolar coupling is the dominant type of spin-spin interaction. These programs have been used to simulate EPR spectra recorded from electron transport particles obtained from beef heart mitochondria[1] and from an intermediate species rapidly formed in the reaction of the vitamin B_{12} requiring enzyme, diol dehydrase, with its substrate[2]. The assumptions involved in the programs and the spectra calculated will be discussed and compared with the experimental observations.

1. F. J. Ruzicka, et al., in preparation.
2. J. E. Valinsky, et al., J. Am. Chem. Soc. 96, 4709 (1974) and references therein.

F-AM-K4 THERMODYNAMIC PARAMETERS OF THE NADH FOLDING REACTION IN AQUEOUS AND METHANOLIC SOLUTIONS AS DETERMINED BY INTRAMOLECULAR FLUORESCENCE ENERGY TRANSFER.† T.W. Houk, Department of Physics, Miami University, Oxford, Ohio 45056, and C.F. Walter, University of Texas, Houston, Texas 77025.

The temperature dependence of fluorescence energy transfer from adenine to nicotinamide moieties in NADH is measured in both aqueous and methanolic solutions. Corrected energy transfer versus temperature curves are fitted to the integrated van't Hoff relation employing the method of MacDonald, et al. (1). Values of the derived thermodynamic parameters are compared to values obtained by NMR chemical shifts in light of the criterion of Lumry, et al. (2). The behavior of NADH under these circumstances yields further information regarding the multistate nature of the folding reaction.

†This work was supported by a grant from the Robert A. Welch Foundation.

(1) McDonald, G., Brown, B., Hollis, D. and Walter, C.F., Biochemistry, 11, 1920 (1972).
(2) Lumry, R., Biltonen, M. and Brandts. J., Biopolymers, 4, 917 (1966).

F-AM-K5 TWO-DIMENSIONAL PATTERNS OF TISSUE METABOLIC STATES. S. Ji*, B. Chance, F. Welch* and B. Quistorff* (Intr. by T.W. Ji). Johnson Fdn. and Neurosurgery Dept., Univ. Pennsylvania Medical Schl., Philadelphia, PA. 19174 and Biochemistry Dept., University of Copenhagen, Copenhagen, Denmark.

A photographic method for recording two-dimensional patterns of NADH fluorescence of the rat brain in vivo (Chance et al., Science 137:3529, 1962) and in freeze-trapped samples (Chance et al., These Abstracts, TE-8, 1963) has been developed. Excitation light at 366 nm is provided by a 100 W water-cooled Hg arc with Corning 5840 filter. Fluorescence at 450 nm is recorded by a 35 mm Nikon camera on Kodak Spectrum Analysis film #3 through Wratten 2C and #47 filters (Chance et al., Neurosci. Abstr., 1974). Reflectance at 366 nm is measured with the 366 nm pass-filter in order to monitor blood volume changes in the brain (Harbig et al., submitted to J. Appl. Physiol.). For fluorescence photographs, the film is exposed for about 25 sec at f/5.6 and for reflectance photographs, for 10 sec at f/22. The rat brain cortex subject to anoxia typically showed +30% to +50% changes in fluorescence intensity and -8% to -15% changes in reflectance as determined at specific loci by a microdensitometer (6 rats). Taking advantage of the fact that low temperature significantly increases the quantum yield of NADH fluorescence (Chance et al.,1963), we have taken fluorescence photographs of brain slices freeze-trapped by conventional methods or by ultra-rapid cooling (Bolwig and Quistorff, J. Neurochem., 21:1345, 1973). The exposure time for low temperature fluorescence photographs was about 0.5 sec at f/16. These photographs suggest that metabolic mapping in two and ultimately three dimensions is possible.
(Supported by USPHS NINDS 10939)

F-AM-K6 CHANGES IN THE NMR RELAXATION TIMES OF SKELETAL MUSCLE WATER PROTONS AS A FUNCTION OF TIME. D. C. Chang, C. F. Hazlewood, and D. E. Woessner*, Department of Physics, Rice University, Houston, Texas 77005, Departments of Pediatrics and Physiology, Baylor College of Medicine, Houston, Texas 77025, and Field Research Laboratory, Mobil Research and Development Corporation, Dallas, Texas 75221.

Water in biological tissues has been studied with nuclear magnetic resonance techniques in recent years. The relaxation times were found to be significantly different than those of pure water. The difference is attributed by some investigators to the ion-water-macromolecular interactions. Our data recently shows that the water in skeletal muscle involves no less than three different characteristic spin-spin relaxation times (T_2). The spin-lattice relaxation time (T_1) of muscle water also is found to be complex. A detailed study of the T_1 data revealed that the characteristic T_1 curve is a function of the degree of freshness of the muscle sample. If one measures the difference between the average T_1 value and the asymptotic T_1 value (ΔT_1) as a function of time, ΔT_1 will reach a maximum value at about three hours after the animal is killed. The T_2 curve of muscle water also is found to vary with the freshness of the sample. These results appear to indicate that a change in the physiological state of muscle (deterioration) will have certain effects on the properties of tissue water. (Supported by the Robert A. Welch Foundation, Liberty Muscular Dystrophy Foundation, NIH #GM-20154, and the ONR #N0014-75-A-0017.)

F-AM-K7 C-13 NMR RELAXATION TIMES OF ISOTOPE-ENRICHED GLYCINE IN FROG MUSCLE. Margaret C. Neville and Herman R. Wyssbrod. University of Colorado Medical Center, Denver, Colorado 80220 and Mount Sinai School of Medicine, New York, New York 10029.

Longitudinal relaxation times (T_1) of 90% ^{13}C enriched glycine accumulated in frog muscle were determined at 1°C at 22.63 MHz and compared with those obtained in free solution. The T_1 value for the C^{α} of [$^{13}C^{\alpha}$] glycine in frog muscle (1.1 sec) was about 50% of that observed in free solution (2.1 sec) and was not concentration dependent. The T_1 value for the C' of 15.9 mM [$^{13}C'$] glycine in muscle (14 sec) was about 67% of that of a 20 mM solution (22 sec). These observations indicate that ^{13}C NMR relaxation times can be obtained for enriched compounds accumulated within biological tissues at concentrations near the normal physiological range. The results provide no evidence for substantial binding of glycine by frog muscle at 1°C and are consistent with a 50% reduction in the diffusion constant of glycine within the tissue. (Supported by NIH grant No. AM-15807).

F-AM-K8 RAPID DETERMINATION OF THE MOLECULAR WEIGHT OF DIVERSE MACROMOLECULES FROM DIFFUSION AND VISCOSITY MEASUREMENTS. by A. M. Jamieson and M. McDonnell (Introduced by Dr. J. Goren, University of Calgary, Calgary, Alberta, Canada) Department of Macromolecular Science, Cleveland, Ohio 44106.

The translational diffusion coefficient and the intrinsic viscosity of a macromolecule are related to the hydrodynamic volume through the Stokes-Einstein relation and the Einstein-Simha equation, respectively. Correlation of these two volume measurements permits a determination of the macromolecular weight. Diffusion coefficients of macromolecules can be measured in a few minutes by quasielastic laser light scattering. Classical methods are used to measure viscosity. For well characterized natural and synthetic macromolecules in different solvents a plot of $M \cdot [\eta]$ as a function of $D^{o} \cdot \eta/T$ (where M is the molecular weight; $[\eta]$, the intrinsic viscosity; D^{o}, the diffusion coefficient extrapolated to zero concentration; η, the solvent viscosity; and T, the temperature) provides a nearly universal curve; the goodness of the solvent enters only weakly. This plot permits a quick method for determining the molecular weight of fairly monodisperse fractions of macromolecules or complexes. The procedure is used to find the molecular weight of polysaccharides and native and denatured proteins. This work was sponsored by USPHS under grant number NIHD 00669.

F-AM-K9 ELECTRON SCATTERING MEASUREMENTS USED TO DETERMINE THE MASS OF VIRUSES. M. K. Lamvik*and D. B. Furlong,*Departments of Biophysics and Microbiology and Enrico Fermi Institute, University of Chicago, Chicago, Illinois 60637. (Intr. by M. S. Isaacson)

There are known relationships between the number of electrons scattered from an object and the number and type of atoms of which the object is made. If the object is sampled at all points by an electron beam that is very small compared to the observed object, then the mass density may be computed at each point, and the total mass obtained by simple integration. Such measurements are being done in the scanning transmission electron microscope of A. V. Crewe (1). This technique is valid over a much greater thickness range than conventional "Quantitative Electron Microscopy," which integrates optical transmission of the micrograph rather than detecting electron scattering directly. To utilize this technique it is essential to determine to what extent the objects under observation lose mass due to the action of the incident electrons. Preliminary measurements at 30 kv indicate that herpesviruses lose less than 10 per cent of their mass after a dose of 1.5 electrons/A^2. Five separate measurements may be done before this dose is reached, indicating that mass loss is sufficiently small to allow extrapolation back to the pre-exposure mass. After a large dose the viruses may lose more than 50 per cent of their initial mass. Accurate averages are obtained by measuring large numbers of particles.

(1) J. Wall, J. Langmore, M. Isaacson and A. V. Crewe, P.N.A.S. 71, 1 (1974).

F-AM-K10 SEPARATION OF RED CELLS INTO AGE GROUPS BY COUNTERFLOW CENTRIFUGATION. R.J. Sanderson*, Webb-Waring Lung Institute, University of Colorado Medical Center, 4200 E. 9th Avenue, Denver, Co. 80220, N.F. Palmer* and Karyn E. Bird*, Children's Hospital, Denver, Co. Intr. by M.L. Morse.

Populations of human red blood cells were separated into fractions of constant age using the technique of counterflow centrifugation. The centrifuge head used was the Beckman Elutriator with a specially designed chamber. Assays of the activity of glutamate-oxalacetate transaminase and measurements of cell volume distribution obtained from a Coulter counter were used to determine the efficacy of the separation technique. The principles of the design of the chamber are given.

F-AM-K11 LOW-ANGLE X-RAY DATA PROCESSING FOR COLLAGEN
S. K. Wang and C. R. Worthington, Departments of Biological Sciences and Physics, Carnegie-Mellon University, Pittsburgh, Pennsylvania

In the study of biological structure by X-ray diffraction the observed intensities are multiplied by a correction factor C(h) to obtain the correct Fourier transform. An analysis for C(h) for a cylindrical specimen (radius r) with an axial repeating structure. The combined effects of specimen disorientation, curvature of the reflection sphere and the divergence of the incident beam are considered. The correction factor C(h) is given by:

$$C(h) = \left(R^2 + h^2\omega^2/d^2 + h^2\epsilon^2/d^2\right)^{1/2} \exp\left[\Delta^2\left(R^2 + h^2\omega^2/d^2 + h^2\epsilon^2/d^2\right)^{-1}\right] \quad (1)$$

where R is the radius of the disc in reciprocal space and r R $\approx$ 1, d is the axial period, h is the order of diffraction, ω is mean angle of disorientation, ϵ is the mean angle of beam divergence and Δ is the deviation of the reflection sphere from the center of the disc and is a function of h. From (1) C(h) depends on ω, ϵ and R. The value of r (and R) can be obtained by experiment. In case of wet collagen it has been found that r $\approx$ 1000 Å and the effects of ϵ and Δ can be neglected. For small h, C(h) $\approx$ 1 but for large h, C(h) > 1. In case of wet elastoidin it is found that r $\gtrsim$ 1 μ and elastoidin has no disorientation ie., ω = o. In this case C(h) is large for large h. In practice, it is usual to tilt the specimen so that the center of the disc cuts the reflection sphere ie., Δ = o, but correction for beam divergence is still needed.

F-AM-K12 THREE-DIMENSION RECONSTRUCTION OF IMAGES FROM THE ACTA-SCANNER.
H. K. Huang, Menfai Shiu*, National Biomedical Research Foundation, Georgetown University Medical Center, Washington, D.C. 20007.

The ACTA-Scanner (Automatic Computerized Transverse Axial) is a tomographic x-ray scanner which can scan successive cross sections everywhere on the whole body and reconstruct the corresponding images as digital pictures. Each cross section has a thickness of 7.5 mm and its reconstructed image consists of a raster of 160 x 160 picture points. The value of each picture point represents the relative absorption coefficient of a corresponding 1.5 x 1.5 mm^2 area of the cross-section.

After a cross-sectional scan, the pathology can be isolated automatically if it has distinct boundaries or manually otherwise. This information can be saved on magnetic tape for the next step in the reconstruction algorithm. This procedure repeats itself until all the necessary cross sections have been scanned.

The pertinent data relating to the pathology under consideration of each cross section can be read back into the computer memory of the ACTA system and a computer program then aligns all the cross sections into proper order. The gap between two cross sections can be filled in by using the principle of interpolation. The three-dimensional reconstruction of the pathology is then complete.

In order to visualize any oblique cross section of the reconstructed three-dimensional image, a computer program selects the proper coordinates pertinent to that section and projects the image on a TV screen. The reconstruction procedure can be on-line and/or off-line.

F-AM-K13 DETERMINATION OF INTRACELLULAR CHLORIDE IN BALANUS EBURNEUS PHOTORECEPTOR. James H. Saunders and H. Mack Brown, Departments of Physiology and Medicine, University of Utah College of Medicine, Salt Lake City, Utah 84132.

Using a new Ag/AgCl microelectrode, we have found that chloride is passively distributed in the dark-adapted Balanus photoreceptor ($E_m = E_{Cl}$); this is in agreement with previous measurements with a Cl^- ion-exchanger microelectrode. However, chloride washout appears to be more complete and faster with the Ag/AgCl electrode than when measured with the liquid ion-exchanger. In two-component mixed solutions at constant ionic strength (e.g. HCO_3^- + Cl^- = 100 mM) liquid ion-exchanger microelectrodes always overestimate a_{Cl} as chloride is replaced by the test anion. This has been shown for those anions which might be expected to comprise part of the intracellular "fixed anion pool;" i.e. HCO_3^-, propionate$^-$, isethionate, Br^- and I^-, and some anions which might be desirable as extracellular chloride substitutes, e.g. methanesulfonate. The problem is far more complex in multi-component systems, i.e. in the cell, and is further complicated by the fact that the calculated selectivity coefficients for the liquid exchanger are not constant at constant ionic strength. This research was supported by USPHS Grant EY00762.

F-AM-L1 CHOLESTEROL ESTER PHASE TRANSITIONS IN HUMAN SERUM LOW DENSITY LIPOPROTEINS R.J. Deckelbaum*, G.G. Shipley, R.S. Lees*, and D.M. Small, Boston U. Med. Ctr. and M.I.T., Boston, MA. 02118

X-ray scattering patterns of intact human serum low density lipoprotein (LDL) at 20°C are typical of a spherical particle with non-uniform electron density distribution but contain an intense maximum corresponding to a Bragg spacing of 36Å. This maximum disappears above 40°C, leaving the remainder of the x-ray scattering profile essentially unaltered. The 36Å spacing returns on cooling to 20°C. Using differential scanning calorimetry, a broad reversible thermal transition has been found in LDL between 20 and 44°C. When expressed in terms of LDL cholesterol ester (CE), the enthalpy (ΔH) of this transition is 0.8 cal/g CE. The transition temperatures and ΔH approximate those of the liquid crystalline-liquid phase transitions in model CE systems. If the LDL is denatured by heating to 100° and re-examined at 20°C, all the low angle maxima disappear with the exception of the 36Å spacing. This spacing is temperature dependent and parallels its behaviour in intact LDL. Total CE isolated from LDL has a liquid crystal-liquid transition in the same temperature range as the transition in intact LDL. Further, the smectic liquid crystal state of the isolated CE gives a single diffraction line at 36Å which disappears above the transition. The same spacing and temperature dependence is found in mixed smectic liquid crystal solutions of cholesteryl oleate and linoleate, the predominant CE's of LDL. We conclude that the transition in intact LDL is due to a CE liquid crystal-liquid transition and that the 36Å spacing results from LDL CE being in a liquid crystalline state below the transition. Thus, a CE rich region(s) exists within the LDL particle large enough to permit a layered liquid crystal arrangement capable of a co-operative melting transition.

F-AM-L2 ENZYMIC FORMATION OF 6-OXO-BENZO(a)PYRENE RADICAL FROM CARCINOGENIC BENZO(a)PYRENE. S.Lesko, W.Caspary*, R.Lorentzen*, and P.Ts'o, Johns Hopkins University, Baltimore, Maryland 21205.

Upon incubation of benzo(a)pyrene (BP) in rat liver homogenates at 37°, an ESR signal was generated, extracted into benzene, and identified as the 6-OXO-BP radical by its characteristic hyperfine structure. The incubation mixture in 30 ml volume contains 88mM niacinamide, 0.22mM NADP, 5mM glucose-6-P, 0.19-0.67mM BP, 0.6% KCl and 0.05M K phosphate (pH 7.4). Formation of radical depended on a NADPH generating system; no radical was observed in heated homogenates. B(e)P did not give an ESR signal. The radical conc. peaked at ~14 min. and declined rapidly to a low level at 20 min. Oxidation of 6-OH-BP in liver homogenates was non-enzymic and followed first order kinetics with a rate constant of 0.29 $min.^{-1}$ and a half-life of 2.4 min. Total ^3H-BP hydroxylation in 1 ml incubation mixtures at conditions described above was determined by measuring formation of ^3H_2O. This hydroxylation followed zero-order kinetics over the first 10 min. Rate constants per mg protein are 1.5×10^{-8} and 0.7×10^{-8} moles/liter-min. for Sprague-Dawley and ACI rats, respectively. The amount of BP metabolized through 6-OH-BP was estimated by measuring 6-OXO-BP radical conc. after a selective oxidation of 6-OH-BP with 2,6-dichloroindophenol. The rate of formation of 6-OH-BP was measured and corrected for its autooxidation. The rate constants per mg of protein were 2×10^{-9} and 1×10^{-9} moles/liter-min. for Sprague-Dawley and ACI rats. The formation of 6-OH-BP was found to represent 13% and 14% of total liver metabolism of BP in Sprague-Dawley and ACI rats. The data indicate that 6-OH-BP is a major metabolite of BP and could be a possible candidate as an "ultimate or proximate carcinogen" because of its reactivity. Supported by AEC contract No. AT(11-1) 3280 and NCI grant No. 5 R01 CA13370.

F-AM-L3 CYCLIC NUCLEOTIDE BINDING PROTEINS IN RAT MAMMARY GLAND NUCLEAR EXTRACTS CONTAINING PROTEIN KINASES AND DNA-DEPENDENT RNA POLYMERASES.
K.M. Anderson, P.J. Doherty*, Department of Clinical Biochemistry, University of Toronto, Toronto, M5G 1L5, Ontario, Canada.

Nuclear extracts from rat mammary glands contain cyclic nucleotide binding activity which was precipitated by ammonium sulfate, non-dialyzable and sensitive to heat or digestion with pronase. Binding of ^{3}H-cyclic AMP could be saturated. Retention of either labelled cAMP or cGMP in the presence of a 10 or 100-fold excess of the other unlabelled nucleotide was reduced by 50 to 98%. From 5-10% of the binding was stable to hot or cold 5% TCA and distributed in several regions after polyacrylamide gel electrophoresis of incubated nuclear extracts. Evidence for "cryptic" binding sites was obtained from studies of stability at 2° and binding in the presence of $(NH_4)_2SO_4$. Nuclear extracts, pre-incubated with ^{3}H-cAMP and chromatographed on DEAE Sephadex, exhibited a number of fractions associated with radioactivity (to 0.15 M $(NH_4)_2SO_4$). Extracts first chromatographed and then incubated with either labelled cyclic nucleotide exhibited a more complex pattern of binding. In addition, two major and 3-5 minor protein kinases were present. Incubation of solubilized RNA polymerase I (nucleolar) and II (nucleoplasmic enzyme) with cAMP increased and decreased, respectively, their apparent activities; cGMP increased the activity of enzyme II. Thus cyclic nucleotides exerted a reciprocal effect on the apparent activity of enzyme II. The relationship between the presence in column fractions of protein kinases, cyclic nucleotide binding proteins, specific RNA polymerases and the changes in their apparent activity due to cyclic nucleotides is not established, but is under study.

F-AM-L4 DEVELOPMENT ASSOCIATED CHANGES IN AVIAN ERYTHROCYTE PHOSPHORYLATED INTERMEDIATES USING ION-EXCHANGE COLUMN CHROMATOGRAPHY.
T.A. Borgese and L.M. Lampert*, Biology Department, Lehman College-CUNY Bronx, New York 10468.

Ion exchange column chromatographic procedures have been used to isolate and quantify changes in specific phosphorylated intermediates in the red cells of the white Peking duck. Unlike mammals and other vertebrates, one of the interesting features of the avian red cell is the fact that it contains virtually no measurable amounts of 2,3 diphosphoglyceric acid (2,3 DPG), the intracellular intermediate presumed to function as an allosteric regulator of oxygen binding to hemoglobin. Instead, significant amounts of inositol hexaphosphate (IHP) can be extracted from chicken, pigeon and, in our laboratory, from duck erythrocytes using Oshima's ferric phytate precipitation procedure. In the present experiments, we have extended our studies to include an analysis of selected phosphorylated intermediates such as inorganic phosphate (Pi), adenosine triphosphate (ATP) and IHP. Neutralized trichloracetic acid extracts of duck red cells containing these intermediates were adsorbed on 1 x 18 cm anion exchange columns which had been converted to the formate form. Four liters of a linear gradient (0 -5 N formate buffer pH 3.0) were passed through the column. IHP was eluted by the subsequent direct application of 1 L of 5 N formate buffer pH 3.0. In replicate experiments, the average values for Pi, ATP and IHP, expressed as phosphorus, were 1.70, 9.58 and 25.6 um / ml cells respectively. Our studies indicate higher levels of Pi and ATP but lower values for IHP in the duckling. While the concentration of IHP-P is nearly halved, the concentration of ATP-P is nearly doubled. The significance of these changes is not clear but may be related to the oxygen requirements of the developing duck. (Supported by NSF Grant to Lehman College.)

F-AM-L5 OPENING OF THE BLOOD-BRAIN BARRIER (BBB) BY A PULSE OF HYDROSTATIC PRESSURE. S.I. Rapoport and H.K. Thompson*, Laboratory of Neurophysiology, National Institute of Mental Health, Bethesda, MD 20014.

The BBB is due to the restricted permeability of cerebral blood vessels to intravascular tracers like Evans blue-albumin. It can be opened by elevating systemic blood pressure with metaraminol, or by shrinking vascular endothelial cells osmotically and widening interendothelial tight junctions (Brightman et al., J. Comp. Neurol. 152, 317, 1973). We show here that elevation of carotid artery pressure in the rat for as short as 3 1/2 sec can open the barrier on the homolateral side of the brain. The common carotid artery was catheterized for brain perfusion, and the external carotid ligated. Perfusion rates were between 0.2 and 0.95 ml/sec and perfusion duration was 3 1/2, 10 or 45 sec. Carotid artery pressure was measured with a pressure transducer before perfusion, and during perfusion after subtracting the pressure drop due to flow through the catheter system. Carotid artery pressures above 200 mm Hg produced extravasation of intravascular Evans blue-albumin within the homolateral hemisphere. The amount of extravasation for a given carotid pressure was greater at 10 and 45 sec perfusion duration than at 3 1/2 sec. The rapid elevation in vascular pressure dilates the cerebral blood vessels, and may physically stress and thereby widen interendothelial tight junctions.

F-AM-L6 ON THE USE OF UNCONVENTIONAL NEGATIVE STAINS FOR THE STUDY OF MACROMOLECULAR ULTRASTRUCTURE. W. H. Massover, Division of Biological and Medical Sciences, Brown University, Providence, Rhode Island 02912.

The chemical agents currently used as negative stains for electron microscopy have at least two properties in common: (1) they contain heavy metal atoms, and (2) they have relatively large amounts of complexed water. These stains are used for macromolecular imaging not only to provide contrast, but also to maintain specimen substructure throughout the preparatory dehydration necessary for high resolution microscopy. By sacrificing the amount of contrast, which is often overwhelming anyway, it might prove feasible to use lighter agents which have better qualities in other important aspects, such as (1) more faithful preservation of the fully hydrated ultrastructure, (2) decreased chemical and physical interactions with the wet specimens, (3) smaller size, such that very small cavities and other details at the level of tertiary or even secondary structure could be imaged, and (4) reduced susceptibility of both the specimen and the stain to damage from electron irradiation. Several unconventional agents, all of which contain no atoms heavier than sulfur, thus far have been recognized as potentially valuable negative stains during the present search. In all cases, washing the specimens with distilled water after their staining has shown that these agents are functioning as bonafide negative stains. Each of these can preserve the ultrastructure of dehydration-sensitive catalase crystals to varying degrees. One agent, containing sodium as its heaviest component, permits the unambiguous identification of apoferritin among unfractionated populations of ferritin macromolecules. (Supported in part by USPHS Biomedical Sciences Support Grant RR-07085-09).

F-AM-L7 REPLICAS OF WATER DROPLETS. Samarendra Basu and D. F. Parsons, Electron Optics Lab., Roswell Park Memorial Institute, Buffalo, N.Y. 14203.

This report concerns a proof of the penetration of the SiO molecular beam used for forming a surface replica through a water vapor layer (1.5mm thick) in a differentially pumped hydration chamber (DPHC) and the ability of SiO to form a coherent layer on water surfaces. The application of this technique for replication of wet biological surfaces was introduced in the previous meeting (1). This new replica technique has been found well suited for studies of nucleation of water droplets on hydrophobic carbon substrate in the submicron droplet range and above. Thus, this method adds a new approach to atmospheric science research on cloud formation. The water droplets have been formed on hydrophobic grids in various ways. First, a large number of droplets in the submicron range (median dia. 0.09-0.13 μm) were formed when the DPHC was operated with supersaturated water vapor. The replicas were made and the size distribution of droplets were measured after a fixed time interval for supersaturation of ΔP_{H_2O}Torr. (increase above equilibrium) from +5 to +12.5 Torr. Control grids using slight undersaturation (ΔP_{H_2O} = -5 Torr) showed no drops. Secondly, sonicated water-iso-octone emulsions were either settled as drops, or sprayed on dry grids. After iso-octone had volatilized away inside a humidity chamber, the grids were replicated inside the DPHC at equilibrium water vapor pressure. These replicas showed a wide distribution of droplet diameters below and above one micron. (Supported by USPHS Grant No. CA 13845-02 A2).

(1). Samarendra Basu and D.F. Parsons (1974). Federation Proceedings Abst. #589, Biochem/Biophys. Meeting, Minneapolis, Minn. June 2-7.

F-AM-L8 THE MODULATION CONTRAST MICROSCOPE. R. Hoffman* and L. Gross, Department of Microscopy, Waldemar Medical Research Foundation, Woodbury, New York 11797.

A new microscope system has been developed with which transparent objects, living unstained cells, can be observed in detail with unexampled clarity. Existing microscopes can be converted readily to this new viewing system, modulation contrast, by the addition of a modulator in the Fourier plane in back of the objective, on which is imaged a source aperture. Observation of living transparent organisms such as protozoa, metazoa, fish embryos, has required phase contrast and interference contrast microscopes until now; such observation can be made more simply with modulation contrast techniques. Modulation contrast eliminates obscuring halo, an ever present artifact in phase contrast. The image produced by modulation contrast has a 3-dimensional appearance and short depth of focus, permitting different levels of the cells to be in sharp focus. Thus, one can observe the cilia on the surface of the cell, for example, without the organelles inside the organism obscuring the view. Focusing lower into the specimen reveals, in turn, vacuoles, nucleus, and granules without disturbance from structures above or below. Modulation contrast produces images in color equivalent to interference contrast, but with bold relief and 3-dimensionality. Biological specimens viewed under modulation contrast will be compared with those viewed under ordinary microscopy and phase contrast. Modulation contrast is especially suited to viewing tissue and cell cultures in situ.

F-AM-L9 DIFFERENTIAL LASER LIGHT SCATTERING FROM CULTURED HUMAN FIBROBLASTS. by A. M. Jamieson, I. A. Schafer* and A. G. Walton, Department of Macromolecular Science, Case Western Reserve University and Department of Pediatrics, Metropolitan General Hospital, Cleveland, Ohio 44106.†

Current methods of prenatal diagnosis of metabolic disorders of infancy are time-consuming. We have been attracted by the possibility of using differential light scattering (1) as a means of rapidly identifying aberrant cells in amniotic fluid for diagnostic purposes. As a preliminary step, we have studied the differential light scattering patterns of six cultured human fibroblast lines using a Science Spectrum Differential I photometer. The cells were removed from culture by pronase treatment to give rounded cells (2). The cells were (i) a normal control cultured for 2 years, (ii) a normal control cultured for 50 days, (iii) fibroblasts from the same source as (i) and (ii) chemically modified to produce a phenotype of Gaucher's Disease and (iv), (v) and (vi) fibroblasts from three important glycosaminoglycan storage diseases each cultured for times comparable to (ii) and (iii). The two normal fibroblast lines gave similar light scattering patterns but significant differences were observed between the normal cells and the abnormal cells which have large cytoplasmic inclusions.

† Supported by USPHS under grant number 05996 from NICHHD.

1. A. Brunsting and P. F. Mullaney, Biophys. J., 14, 439 (1974).

2. J. C. Sullivan and I. A. Schafer, Exp. Cell. Res., 43, 676 (1966).

F-AM-L10 STUDY OF THE STRUCTURAL BONDING FORCES ON BACTERIOPHAGE T2. R. J. Smith, Dept. of Medical Physics, Memorial Hospital, New York, N. Y. 10021, and S. F. Cleary, Dept. of Biophysics, Virginia Commonwealth University, Richmond, Va.

The present study deals with an investigation of the effects on bacteriophage T2 particles produced by rapid heating of an Oil Blue N dye solution in carbon tetrachloride when a ruby laser light is absorbed by the dye. The ruby laser emits a single pulse of 694.3 nm light of approximately 0.8 J with a pulse width of 3×10^{-8}s. The effects of variation in infectivity and structure on bacteriophage T2 particles caused by variation in urea concentration, hydrogen ion concentration and solvent environment have also been investigated.

The electron microscope was used to ascertain the nature of the damage caused by the acoustic transients.

Theoretical calculations were made to determine the magnitude of the force produced in a bacteriophage T2 particle by an acoustic transient induced by a laser light intensity of 2×10^{12} W/m^2 incident on the dye solution. The magnitude of the force was found to be on the order of 1.3×10^{-4} dynes.

F-AM-L11 THE DISTRIBUTION OF BACTERIA IN THE VELOCITY GRADIENT CENTRIFUGE. A.L. Koch and G. Blumberg*, Department of Microbiology, Indiana, University, Bloomington, Indiana 47401.

Cells in different parts of the cell cycle can be separated by brief centrifugation in a density stabilized gradient: The Vincent Mitchison technique. The position of a cell in the tube depends on the size, shape and density of the cells as well as the density and viscosity of the medium in all centripetal parts of the gradient and time and centrifugal force. A program to compute the velocities and integrate the velocity profile for particles of a particular size class has been developed. Because enteric bacteria are of a form intermediate between right cylinders and prolate ellipsoids of revolution, the program uses an intermediate value of the frictional coefficient from those calculated from formulas for ellipsoids or cylinders. The formula $f=6\pi\eta b\sqrt{a/b}$ possesses this property and because of its simplicity greatly speeds the calculations. A second program computes the frequency of bacterial mass or number class. It takes into account the known variation of cell size of those organisms in the act of cell division. It also computes the distribution of organisms in each sedimentation velocity, or s class. Use of the expression given above for f allows analytical transformation of the idealized distributions which are combined to take into account cell size at division. The two programs in conjunction compute the mass or cell number profile in any arbitrary gradient. The program has been used to design gradients to maximize the resolution of the technique. Work supported by USPH grant AI-09337 and NSF GB-32115.

F-AM-L12 AN EVALUATION OF INFORMATION DERIVED FROM GROWTH CURVES OF SOLID TUMORS FOLLOWING RADIATION. J.S. Trefil*, J.G. Schaffner*, C.J. Kovacs* and W.B. Looney, Division of Radiobiology and Biophysics and Department of Physics, University of Virginia, Charlottesville, Virginia 22901.

The ability to quantitatively evaluate the response of experimental solid tumors to different modalities of treatment has important implications for devising more effective treatment schedules for cancer patients. A computer program has been developed to quantitatively evaluate changes in tumor growth rates following a series of radiation doses (375-3750 r). Since 3750 r results in tumor regression, it has been possible to quantitatively evaluate these parameters over the entire spectrum of radiation induced changes on tumor growth rates. By a method of least squares, the non-linear tumor growth response to increasing radiation doses was evaluated. This method has been extended to obtain information about: (a) the average growth rates of viable cells; (b) the delay time prior to the removal of tumor cells following radiation; and (c) the proliferative and non-proliferative population size as a function of dose. Furthermore, this program permits quantitative comparisons between the response of this tumor model to both radiotherapy and chemotherapy. The clinical implications of these findings will be discussed. This investigation was supported by Public Health Service Research Grants Nos. CA-12758 and CA-13102 from the National Cancer Institute.

F-AM-L13 MICROSCOPIC FLUCTUATIONS SPECTROSCOPY. Z. Kam, Department of Physics, University of California, San Diego, La Jolla, CA 92037.

Quasielastic light scattering (QELS) correlates fluctuations in refractive index among regions of the order of the wavelength of light. Thus, in principle, QELS should be applicable to studies of *in vivo* processes (e.g., diffusion, self-assembly) within a single cell. In order to test the feasibility of such experiments we studied theoretically and experimentally model systems. A microscope was used to image the illuminated area with high magnification, and an aperature in front of the photomultiplier defined the scattering region. Factors that have to be considered in attempting to extend the QELS technique for scattering regions of several microns in size are: (1) Microscope objective aperature has to be large to resolve small objects, hence the light is collected in a wide range of scattering vectors, K. (2) The small scattering region introduces large coherence areas and an additional uncertainty in K. (3) Diffusion in and out of the scattering volume introduces number fluctuations. We found that for a numerical aperature of .75, one can easily resolve a region with dimensions of a few microns. Due to the spread in the K vectors, the observed diffusional linewidth is about half its value for 90° scattering and the lineshape deviates slightly (although systematically) from a Lorentzian. The uncertainty in K for a particular angle of scattering is only a few percent and the collecting aperature angle includes a few coherence areas. Since the wavelength of light is an order of magnitude shorter than the length of the scattering region, the characteristic frequency for number fluctuations is two orders of magnitude below the diffusional fluctuations frequency. In addition, the integrated power spectrum due to number fluctuations can be neglected whenever the number of coherence areas collected is much smaller than the number of scattering particles. Work supported by NIH grant GM-13191.